Quark mean field model with pion and gluon corrections for Λ and Ξ^0 hypernuclei and neutron stars

Xueyong Xing, Jinniu Hu,* and Hong Shen
School of Physics, Nankai University, Tianjin 300071, China
(Received 21 March 2017; published 15 May 2017)

Properties of Λ and Ξ^0 hypernuclei and neutron stars are investigated in a quark mean field model with pion and gluon corrections. First, u, d, and s quarks are confined by relativistic harmonic oscillator potentials to generate baryons, such as nucleons and Λ, Σ, and Ξ hyperons. The effects of pion-quark coupling and one-gluon exchange are considered perturbatively. Then, the baryons interact with each other through exchanging σ, ω, and ρ mesons between quarks in hypernuclei and nuclear matter. The strengths of confinement potentials for u, d, and s quarks are determined by the masses and radii of free baryons. The coupling constants between the quarks and mesons are fixed by the ground-state properties of several nuclei and single-hyperon potentials at nuclear saturation density, which yields three parameter sets for the coupling constants between mesons and quarks, named QMF-NK1S, QMF-NK2S, and QMF-NK3S. Compared to the results of the previous quark mean field model without pion and gluon corrections, it is found that properties of Λ hypernuclei, i.e., the single-Λ energies, are more consistent with the experimental observables. Properties of Ξ^0 hypernuclei are also calculated and compared with the results in the previous quark mean field model. With these three parameter sets, the neutron stars containing hyperons are investigated through solving the Tolman-Oppenheimer-Volkoff equation. Maximum masses of neutron stars approach $2.1M_\odot$ with hyperons, and corresponding radii are around 13 km.

DOI: 10.1103/PhysRevC.95.054310

I. INTRODUCTION

With increasing energy and density, the strangeness degree of freedom will appear in nuclear physics to generate hypernuclei and strange nuclear matter, even in the core region of neutron stars. Many large facilities are attempting to produce a lot of experimental data about the hypernuclei to further investigate strangeness nuclear physics, such as J-PARC, MAMI, JLab, FAIR, and so on [1]. Until now, Λ hypernuclei are the most familiar objects in strangeness physics and have rich experimental events, that were largely created in laboratories from ${}^{3}_{\Lambda}$H to ${}^{208}_{\Lambda}$Pb, while it is generally recognized that Σ hypernuclei do not exist except ${}^{4}_{\Sigma}$He. Furthermore, there are only several observed data on Ξ hypernuclei in ${}^{12}\mathrm{C} + \Xi^-$ and ${}^{14}\mathrm{N} + \Xi^-$ systems [2–5].

On the other hand, the theoretical study of hypernuclei has been advancing on the basis of a number of experiments on hypernuclei [6–13]. The light hypernuclei can be described precisely by *ab initio* calculation with a realistic hyperon-nucleon interaction [14]. For the systematic study of both light and heavy hypernuclei, nonrelativistic and covariant density functional theories are generally employed, such as the Skyrme Hartree-Fock (SHF) model [15–19], relativistic mean field (RMF) model [20–23], relativistic point-coupling model [24], and so on.

Since massive neutron stars ($M \sim 2M_\odot$) were observed [25–27], it was found that a large number of available theoretic models, which can describe the properties of hypernuclei very well, lead to too soft equations of state (EOS) with hyperons to satisfy the astronomic observables. This dilemma is called the hyperon puzzle. To solve such a problem, many mechanisms were proposed to introduce an extra repulsion to make the EOS stiffer, such as the inclusion of a more repulsive hyperon-hyperon force [28,29], inclusion of a three-body hyperon force [30], and quark stars [25].

Most of the available nuclear models are based on the understanding of baryons as fundamental particles; however, in quantum chromodynamics (QCD), which is regarded as the standard theory to describe the strong interaction, quarks and gluons are considered fundamental particles. They constitute mesons and baryons such as pions, nucleons, and hyperons. These compound particles combine together to form a nucleus via the baryon-baryon force in terms of the residual part of the strong interaction at the hadron level. The nuclear many-body system cannot be solved directly from QCD theory currently due to its nonperturbative feature at low energies. Therefore, it is very important to consider nucleon structure in a nuclear many-body system in terms of the quark degree of freedom.

A few attempts have been made to study strangeness nuclear physics at the quark level. The quark-meson coupling (QMC) model [31–36] and quark mean field (QMF) model [37–47] are two most successful schemes, where quarks are confined to form a baryon by the MIT bag model and confinement potential model, respectively. The baryons in hypernuclei and strange nuclear matter interact with each other via exchanging σ, ω, and ρ mesons between the quarks in different baryons. The properties of baryons will be changed due to the influence of surrounding baryons, which can explain the medium modification of the nucleon structure function (EMC effect) [48]. However, in these two models, two essentials of QCD theory were not included: chiral symmetry and gluons. At the mean field level, the pion contribution is zero, therefore recently many works have started to consider the pion effect in the QMC model through the exchange term [49–51]. Furthermore, Nagai *et al.* developed the QMC model to include the gluon and pion effects by using the cloudy bag model (CBM) [52].

*hujinniu@nankai.edu.cn

Several years ago, Mishra *et al.* attempted to overcome such difficulties via calculating the contributions of quark-pion and quark-gluon interactions by one-pion and one-gluon exchange terms, within lowest-order perturbation theory in a modified quark meson coupling (MQMC) model [53,54], and they applied such a model to the investigation of strange nuclear matter and neutron stars [55]. They obtained massive neutron stars, whose masses are around $2M_{\odot}$, after fitting the hyperon coupling constants by the empirical Λ-, Σ-, and Ξ-nucleon single-particle potentials at nuclear saturation density. However, in their works, both the coupling constants between the mesons and nucleons and those between mesons and hyperons were determined by the empirical properties of strange nuclear matter at saturation density. Actually, these coupling constants should be also constrained by the properties of normal nuclei and hypernuclei. With coupling constants given by Mishra *et al.*, the properties of nuclei and hypernuclei were not consistent with the experimental data.

In the past few years, we have studied the structures of nuclei and neutron stars in the QMF model with pion and gluon effects [56] following the scheme of Mishra *et al.* It was found that the effects of pion and gluon could improve the description by the QMF model of a nuclear many-body system containing u and d quarks. In the present work, this framework will be extended to include the strangeness degree of freedom to study properties of Λ and Ξ^0 hypernuclei and neutron stars with hyperons and compare with our previous studies on the strangeness system in the QMF model without pion and gluon effects [40,41], where the hyperon binding energies of Λ and Ξ^0 hypernuclei and properties of neutron stars were calculated.

The paper is written as follows. In Sec. II, we briefly derive the formulas of the QMF model with pion and gluon corrections including strangeness degree of freedom. In Sec. III, the new parameter sets of the QMF model with pion and gluon corrections for hypernuclei will be determined. The properties of Λ and Ξ^0 hypernuclei with the new parameter sets will be shown. Neutron stars with hyperons will be investigated also. A summary is given in Sec. IV.

II. QUARK MEAN FIELD MODEL WITH PION AND GLUON CORRECTIONS FOR HYPERNUCLEI AND NEUTRON STARS

The analytical confinement potential for quarks cannot be obtained from QCD theory directly. Many phenomenological confinement potentials have been proposed, where the polynomial forms are widely used. A harmonic oscillator potential mixing scalar and vector Lorentz structures, $U(r)$, is adopted in this work, where the Dirac equation can be solved analytically [56]:

$$U(r) = \tfrac{1}{2}(1+\gamma^0)(a_q r^2 + V_q), \tag{1}$$

where q denotes u, d, or s. When the effect of nuclear medium is considered, the quark field $\psi_q(\vec{r})$ satisfies the following Dirac equation:

$$\begin{aligned}\big[\gamma^0\big(\epsilon_q - g^q_\omega\omega - \tau_{3q}g^q_\rho\rho\big) - \vec{\gamma}\cdot\vec{p} \\ -\big(m_q - g^q_\sigma\sigma\big) - U(r)\big]\psi_q(\vec{r}) = 0,\end{aligned} \tag{2}$$

where σ, ω, and ρ are the classical meson fields, which describe the exchanging interaction between quarks. g^q_σ, g^q_ω, and g^q_ρ are the coupling constants of σ, ω, and ρ mesons with quarks, respectively. τ_{3q} is the third component of isospin matrix and m_q is the bare quark mass. Now we can define the following quantities for convenience:

$$\epsilon'_q = \epsilon^*_q - V_q/2, \quad m'_q = m^*_q + V_q/2, \tag{3}$$

where the effective quark energy is given by $\epsilon^*_q = \epsilon_q - g^q_\omega\omega - \tau_{3q}g^q_\rho\rho$ and the effective quark mass by $m^*_q = m_q - g^q_\sigma\sigma$ [56]. We also introduce λ_q and r_{0q} as

$$\lambda_q = \epsilon'_q + m'_q, \quad r_{0q} = (a_q\lambda_q)^{-\frac{1}{4}}. \tag{4}$$

The baryon mass in nuclear medium can be expressed as the binding energy of three quarks, named the zeroth-order term, after solving the Dirac equation (2), formally

$$E^{*0}_B = \sum_q \epsilon^*_q. \tag{5}$$

The quarks are simply confined in a central confinement potential. Three corrections will be taken into account in the zeroth-order baryon mass in nuclear medium, including the center-of-mass correction $\epsilon_{\text{c.m.}}$, the pion correction δM^{π}_B, and the gluon correction $(\Delta E_B)_g$. The pion correction is caused by the chiral symmetry of QCD theory and the gluon correction by the short-range exchange interaction of quarks. The center-of-mass correction can be expressed by [56]

$$\epsilon_{\text{c.m.}} = \langle B|\mathcal{H}_{\text{c.m.}}|B\rangle, \tag{6}$$

where $\mathcal{H}_{\text{c.m.}}$ is the center-of-mass Hamiltonian density and $|B\rangle$ is the baryon state. When the baryon wave function is constructed by the quark wave functions, the center-of-mass correction comes out as [55]

$$\epsilon_{\text{c.m.}} = e^{(1)}_{\text{c.m.}} + e^{(2)}_{\text{c.m.}}, \tag{7}$$

where

$$e^{(1)}_{\text{c.m.}} = \sum_{i=1}^{3}\left[\frac{m_{q_i}}{\sum_{k=1}^{3} m_{q_k}}\frac{6}{r^2_{0q_i}\big(3\epsilon'_{q_i} + m'_{q_i}\big)}\right],$$

$$\begin{aligned}e^{(2)}_{\text{c.m.}} = \frac{1}{2}\Bigg[&\frac{2}{\sum_k m_{q_k}}\sum_i a_i m_i\langle r_i^2\rangle + \frac{2}{\sum_k m_{q_k}}\sum_i a_i m_i\langle\gamma^0(i)r_i^2\rangle - \frac{3}{\big(\sum_k m_{q_k}\big)^2}\sum_i a_i m_i^2\langle r_i^2\rangle - \frac{1}{\big(\sum_k m_{q_k}\big)^2}\sum_i\langle\gamma^0(1)a_i m_i^2 r_i^2\rangle \\ &- \frac{1}{\big(\sum_k m_{q_k}\big)^2}\sum_i\langle\gamma^0(2)a_i m_i^2 r_i^2\rangle - \frac{1}{\big(\sum_k m_{q_k}\big)^2}\sum_i\langle\gamma^0(3)a_i m_i^2 r_i^2\rangle\Bigg].\end{aligned} \tag{8}$$

Here, the different expectation values related to radii are listed as follows:

$$\begin{aligned}\langle r_i^2\rangle &= \frac{(11\epsilon'_{qi}+m'_{qi})r_{0qi}^2}{2(3\epsilon'_{qi}+m'_{qi})},\\ \langle \gamma^0(i) r_i^2\rangle &= \frac{(\epsilon'_{qi}+11m'_{qi})r_{0qi}^2}{2(3\epsilon'_{qi}+m'_{qi})},\\ \langle \gamma^0(i) r_j^2\rangle_{i\neq j} &= \frac{(\epsilon'_{qi}+3m'_{qi})\langle r_j^2\rangle}{3\epsilon'_{qi}+m'_{qi}}.\end{aligned} \tag{9}$$

In the QMF model, the constituent quark masses are obtained due to spontaneous chiral symmetry breaking. It is then natural to generate nearly zero mass pions such as Nambu-Goldstone bosons. Their coupling to the constituent quarks is provided by the chiral symmetry. In order to treat the chiral symmetry properly in the baryon, an elementary pion field is introduced in the present model. The pionic self-energy correction to the nucleon mass becomes

$$\delta M_N^{\pi} = -\frac{171}{25} I_\pi f_{NN\pi}^2, \tag{10}$$

where

$$I_\pi = \frac{1}{\pi m_\pi^2}\int_0^\infty dk \frac{k^4 u^2(k)}{w_k^2}, \tag{11}$$

with the axial-vector nucleon form factor

$$u(k) = \left[1 - \frac{3}{2}\frac{k^2}{\lambda_u(5\epsilon'_u + 7m'_u)}\right] e^{-\frac{1}{4}r_{0u}^2 k^2}, \tag{12}$$

and $f_{NN\pi}$ can be obtained from the Goldberg-Triemann relation by using the axial-vector coupling-constant value g_A in this model. The pionic corrections for Λ, Σ, and Ξ hyperons become

$$\begin{aligned}\delta M_\Lambda^{\pi} &= -\tfrac{108}{25} f_{NN\pi}^2 I_\pi,\\ \delta M_\Sigma^{\pi} &= -\tfrac{12}{5} f_{NN\pi}^2 I_\pi,\\ \delta M_\Xi^{\pi} &= -\tfrac{27}{25} f_{NN\pi}^2 I_\pi.\end{aligned} \tag{13}$$

The one-gluon exchange contribution to the baryon mass is separated into two parts as

$$(\Delta E_B)_g = (\Delta E_B)_g^E + (\Delta E_B)_g^M, \tag{14}$$

where $(\Delta E_B)_g^E$ is the color-electric contribution

$$(\Delta E_B)_g^E = \frac{1}{8\pi}\sum_{i,j}\sum_{a=1}^{8}\int \frac{d^3r_i d^3r_j}{|\vec{r}_i - \vec{r}_j|}\langle B|J_i^{0a}(\vec{r}_i)J_j^{0a}(\vec{r}_j)|B\rangle, \tag{15}$$

and $(\Delta E_B)_g^M$ the color-magnetic contribution

$$(\Delta E_B)_g^M = -\frac{1}{8\pi}\sum_{i,j}\sum_{a=1}^{8}\int \frac{d^3r_i d^3r_j}{|\vec{r}_i - \vec{r}_j|}\langle B|\vec{J}_i^a(\vec{r}_i)\cdot\vec{J}_j^a(\vec{r}_j)|B\rangle. \tag{16}$$

TABLE I. The coefficients a_{ij} and b_{ij} used in the calculation of the color-electric and color-magnetic energy contributions due to one-gluon exchange for different baryons.

Baryon	a_{uu}	a_{us}	a_{ss}	b_{uu}	b_{us}	b_{ss}
N	−3	0	0	0	0	0
Λ	−3	0	0	1	−2	1
Σ	1	−4	0	1	−2	1
Ξ	0	−4	1	1	−2	1

Here

$$J_i^{\mu a}(x) = g_c\bar{\psi}_q(x)\gamma^\mu\lambda_i^a\psi_q(x) \tag{17}$$

is the ith quark color current density, where λ_i^a are the usual Gell-Mann SU(3) matrices and $\alpha_c = g_c^2/4\pi$. Then Eqs. (15) and (16) can be written as

$$(\Delta E_B)_g^E = \alpha_c\left(b_{uu}I_{uu}^E + b_{us}I_{us}^E + b_{ss}I_{ss}^E\right), \tag{18}$$

and

$$(\Delta E_B)_g^M = \alpha_c\left(a_{uu}I_{uu}^M + a_{us}I_{us}^M + a_{ss}I_{ss}^M\right), \tag{19}$$

where a_{ij} and b_{ij} are the numerical coefficients depending on each baryon and are given in Table I. The quantities I_{ij}^E and I_{ij}^M are given in the following equations:

$$\begin{aligned}I_{ij}^E &= \frac{16}{3\sqrt{\pi}}\frac{1}{R_{ij}}\left[1 - \frac{\alpha_i+\alpha_j}{R_{ij}^2} + \frac{3\alpha_i\alpha_j}{R_{ij}^4}\right],\\ I_{ij}^M &= \frac{256}{9\sqrt{\pi}}\frac{1}{R_{ij}^3}\frac{1}{(3\epsilon'_i+m'_i)}\frac{1}{(3\epsilon'_j+m'_j)},\end{aligned} \tag{20}$$

with

$$\begin{aligned}R_{ij}^2 &= 3\left[\frac{1}{(\epsilon_i'^2 - m_i'^2)} + \frac{1}{(\epsilon_j'^2 - m_j'^2)}\right],\\ \alpha_i &= \frac{1}{(\epsilon'_i+m'_i)(3\epsilon'_i+m'_i)}.\end{aligned} \tag{21}$$

The detailed forms of color-electric and color-magnetic contributions can be found in Ref. [55]. Finally, taking into account all above energy corrections, the mass of a baryon in nuclear medium becomes

$$M_B^* = E_B^{*0} - \epsilon_{\text{c.m.}} + \delta M_B^{\pi} + (\Delta E_B)_g^E + (\Delta E_B)_g^M. \tag{22}$$

Next we would like to connect the baryon in the medium with nuclear objects, such as Λ and Ξ^0 hypernuclei. A single hypernucleus is treated as a system of many nucleons and one hyperon which interact through exchanging σ, ω, and ρ mesons. The QMF Lagrangian in the mean-field approximation can be written as [37–41]

$$\begin{aligned}&\mathcal{L}_{\text{QMF}}\\ &= \bar{\psi}\left[i\gamma_\mu\partial^\mu - M_N^* - g_\omega\omega\gamma^0 - g_\rho\rho\tau_3\gamma^0 - e\frac{(1-\tau_3)}{2}A\gamma^0\right]\psi\\ &\quad + \bar{\psi}_H\left[i\gamma_\mu\partial^\mu - M_H^* - g_\omega^H\omega\gamma^0 + \frac{f_\omega^H}{2M_H}\sigma^{0i}\partial_i\omega\right]\psi_H\end{aligned}$$

TABLE II. The potential parameters (a_q, V_q) obtained for the quark masses $m_u = 250$ MeV, $m_s = 330$ MeV, the quark masses $m_u = 300$ MeV, $m_s = 380$ MeV, and the quark masses $m_u = 350$ MeV, $m_s = 430$ MeV.

	m_u (MeV)	V_u (MeV)	a_u (fm^{-3})	m_s (MeV)	V_s (MeV)	a_s (fm^{-3})
set A	250	−24.286 601	0.579 450	330	101.781 80	0.097 317
set B	300	−62.257 187	0.534 296	380	54.548 210	0.087 243
set C	350	−102.041 575	0.495 596	430	6.802 695	0.079 534

$$-\frac{1}{2}(\nabla\sigma)^2-\frac{1}{2}m_\sigma^2\sigma^2-\frac{1}{3}g_2\sigma^3-\frac{1}{4}g_3\sigma^4+\frac{1}{2}(\nabla\omega)^2+\frac{1}{2}m_\omega^2\omega^2+\frac{1}{4}c_3\omega^4+\frac{1}{2}(\nabla\rho)^2+\frac{1}{2}m_\rho^2\rho^2+\frac{1}{2}(\nabla A)^2, \tag{23}$$

where H denotes Λ or Ξ^0 hyperon and the effective masses of baryons, M_N^* and M_H^*, are generated from the quark model, Eq. (22). These effective baryon masses are actually related to scalar mesons in the RMF model. Furthermore, we should emphasize that the nonlinear terms of σ and ω are included additionally in the present work, compared with the Lagrangian of the MQMC model [54,55], since these terms can largely improve the descriptions of properties of finite nuclei, as shown in our previous work [56]. The tensor coupling between the ω meson and baryons, $\frac{f_\omega^H}{2M_H}\sigma^{0i}\partial_i\omega$, can improve the description of small spin-orbit splittings of hypernuclei [20,21].

The equations of motion of baryons and mesons are obtained by using the Euler-Lagrange equation. Dirac equations for nucleons and hyperons have the following form:

$$\left[i\gamma_\mu\partial^\mu - M_N^* - g_\omega\omega\gamma^0 - g_\rho\rho\tau_3\gamma^0 - e\frac{(1-\tau_3)}{2}A\gamma^0\right]\psi = 0,$$
$$\left[i\gamma_\mu\partial^\mu - M_H^* - g_\omega^H\omega\gamma^0 + \frac{f_\omega^H}{2M_H}\sigma^{0i}\partial_i\omega\right]\psi_H = 0. \tag{24}$$

The equations of motion for mesons are given by

$$\begin{aligned}\Delta\sigma - m_\sigma^2\sigma - g_2\sigma^2 - g_3\sigma^3 &= \frac{\partial M_N^*}{\partial\sigma}\langle\bar\psi\psi\rangle + \frac{\partial M_H^*}{\partial\sigma}\langle\bar\psi_H\psi_H\rangle,\\ \Delta\omega - m_\omega^2\omega - c_3\omega^3 &= -g_\omega\langle\bar\psi\gamma^0\psi\rangle - g_\omega^H\langle\bar\psi_H\gamma^0\psi_H\rangle\\ &\quad + \frac{f_\omega^H}{2M_H}\partial_i\langle\bar\psi_H\sigma^{0i}\psi_H\rangle,\\ \Delta\rho - m_\rho^2\rho &= -g_\rho\langle\bar\psi\tau_3\gamma^0\psi\rangle,\\ \Delta A &= -e\langle\bar\psi\frac{(1-\tau_3)}{2}\gamma^0\psi\rangle.\end{aligned} \tag{25}$$

Here, the coupling constants between ω,ρ mesons and nucleons, g_ω and g_ρ, are generated from quark counting rules, $g_\omega = 3g_\omega^q$ and $g_\rho = g_\rho^q$, while those between ω mesons and hyperons, g_ω^H and f_ω^H, will be determined by the properties of hypernuclei and strange nuclear matter at nuclear saturation density. The above equations of motion of baryons and mesons can be solved self-consistently with numerical methods. From the single-particle energies of nucleons and hyperon, the total energy of whole hypernucleus can be obtained with the mean field approximation.

In strange nuclear matter including Λ, Σ, and Ξ hyperons, the gradient terms in the equations of motion of mesons would disappear. The energy density and pressure are generated from the energy-momentum tensor related to the QMF Lagrangian. In neutron stars, there are not only baryons but also leptons, such as electrons and muons. The neutron star matter satisfies electric neutrality and β equilibrium. In such case, the EOS can be solved and taken into the Tolman-Oppenheimer-Volkoff

TABLE III. The masses of three hyperons (Λ, Σ^0, and Ξ^0) in free space from set A, set B, and set C, compared with the experimental data and the contributions of center-of-mass, pionic, and gluonic corrections to the hyperon masses respectively (the units of all quantities are MeV).

	Baryon	E_B^0	$\epsilon_{\text{c.m.}}$	δM_B^π	$(\Delta E_B)_g$	$M_B^{\text{Theor.}}$	$M_B^{\text{Expt.}}$
set A	Λ	1446.340	231.975	−65.172	−24.390	1124.803	1115.683 ± 0.006
	Σ^0	1446.340	231.975	−36.207	10.515	1188.673	1192.642 ± 0.024
	Ξ^0	1504.254	175.047	−16.293	−1.289	1311.625	1314.86 ± 0.20
set B	Λ	1433.489	220.692	−69.277	−18.313	1125.207	1115.683 ± 0.006
	Σ^0	1433.489	220.692	−38.487	13.753	1188.063	1192.642 ± 0.024
	Ξ^0	1491.611	165.564	−17.319	2.979	1311.707	1314.86 ± 0.20
set C	Λ	1421.908	210.233	−72.829	−13.170	1125.676	1115.683 ± 0.006
	Σ^0	1421.908	210.233	−40.461	16.203	1187.417	1192.642 ± 0.024
	Ξ^0	1480.703	157.102	−18.207	6.377	1311.771	1314.86 ± 0.20

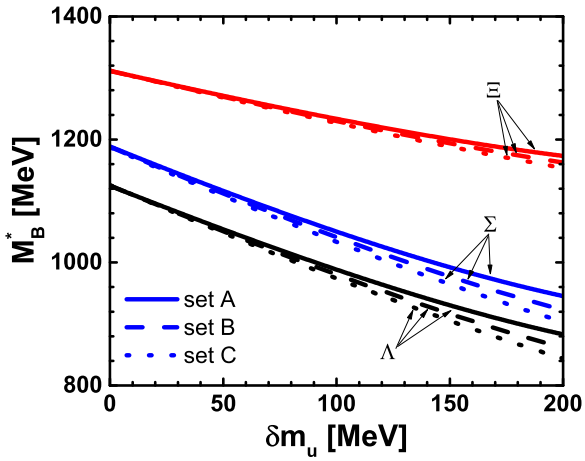

FIG. 1. The effective masses of three hyperons (Λ, Σ, and Ξ) with different parameter sets [set A (solid curve), set B (dashed curve), and set C (dotted curve)] as functions of the u quark mass correction.

(TOV) equation [57,58] to get properties of neutron stars. The detailed formulas can be found in our previous work about the QMF model of neutron stars [41].

III. RESULTS AND DISCUSSION

A. Properties of baryons

Firstly, the strengths of quark confinement potentials for u, d, and s quarks should be determined. In present work, there are two free parameters, a_q and V_q, in the confinement potential for each flavor quark. The differences of properties between u and d quarks are very small, therefore they are treat equally in this work. For the s quark, SU(3) symmetry is broken, where a_s and V_s are distinguished from a_u and V_u. In the QMF model, the quarks are regarded as the constituent ones, whose masses are around 300 MeV for u and d quarks. In recent lattice QCD calculations [59,60], the value of the constituent quark mass was suggested to be around 250–350 MeV. To discuss the influences of quark mass, we take the masses of u and d quarks to be 250, 300, and 350 MeV in three parameter sets. The corresponding a_u and V_u are fixed by the mass and radius of the free nucleon, which were already given in our previous work [56]. The s quark mass and two coefficients, a_s and V_s, in the s quark confinement potential are obtained by fitting the free masses of Λ, Σ^0, and Ξ^0 hyperons [61] through the least-squares method.

These parameters are listed in Table II. For convenience, the first parameter set ($m_u = 250$ MeV) in Table II is named as set A, the second ($m_u = 300$ MeV) as set B, and the third ($m_u = 350$ MeV) as set C. Here, we should emphasize that in the work of Mishra *et al.* [55], each baryon corresponds to one V_q value, while in present work the confinement potentials of the s quark are adopted as having uniform strength in Λ, Σ, and Ξ hyperons. The differences of their masses are generated by the pion and gluon corrections.

In Table III, the masses of three charge neutrality hyperons (Λ, Σ^0, and Ξ^0) in free space with set A, set B, and set C are compared with the latest experimental data [61], respectively. The contributions from center-of-mass, pionic, and gluonic corrections to the hyperon masses in free space are also shown. Under the constraint of the s quark mass, whose value should be larger than those of u and d quarks, the hyperon masses in theoretical calculations do not reproduce the experimental observables [61] from the Particle Data Group completely. There are several-MeV differences between the theoretical prediction and experimental data. The 1% errors are not able to influence the further calculations and discussions.

The behaviors of one baryon in nuclear medium will be influenced by the surrounding particles, therefore its effective mass M_B^* is able to change with increasing density. In the QMF model, the medium effect is included via the effective quark mass generated by the σ meson. Finally, the effective baryon masses are the functions of quark mass corrections $\delta m_q = m_q - m_q^* = g_\sigma^q \sigma$. The σ meson did not contain the strangeness flavor, so that the coupling constant between the s quark and σ meson is zero, i.e., $g_\sigma^s = g_\omega^s = 0$. All effective masses of baryons are only affected by the u and d quarks. In Fig. 1, the effective masses of three hyperons (Λ, Σ, and Ξ) for different parameter sets (set A, set B, and set C) are given as functions of u quark mass correction.

In free space ($\delta m_u = 0$), their effective masses actually correspond to the masses of free hyperons. With δm_u increasing, the effective hyperon masses will be reduced in terms of the effect of surrounding baryons. At small quark mass correction, the effective masses are almost the same for different parameter sets. With the quark mass correction δm_u increasing, the differences among sets A, B, and C becomes obvious for Λ and Σ hyperons. Since there is only one u quark component in the Ξ hyperon, the influences from different parameter sets are very small.

B. Properties of hypernuclei

Once the relation between the effective baryon masses and quark mass corrections is obtained, the next step is to determine the coupling constants between quarks and mesons: g_σ^u, g_ω, g_ω^Λ, g_ω^Ξ, f_ω^H, g_ρ, and the parameters in nonlinear terms of σ and ω mesons, g_2, g_3, and c_3. In this work, the meson masses are taken

TABLE IV. The parameters for quarks and hadrons are listed. The first parameter set corresponding to $m_u = 250$ MeV is named QMF-NK1S, the second for $m_u = 300$ MeV is named QMF-NK2S, and the third for $m_u = 350$ MeV is named QMF-NK3S.

Model	m_u (MeV)	g_σ^u	g_ω	g_ω^Λ	g_ω^Ξ	g_ρ	g_2 (fm^{-1})	g_3	c_3
QMF-NK1S	250	5.158 71	11.547 26	$0.8258 g_\omega$	$0.4965 g_\omega$	3.796 01	−3.527 37	−78.520 06	305.002 40
QMF-NK2S	300	5.093 46	12.300 84	$0.8134 g_\omega$	$0.4800 g_\omega$	4.041 90	−3.428 13	−57.683 87	249.056 54
QMF-NK3S	350	5.016 31	12.838 98	$0.8040 g_\omega$	$0.4681 g_\omega$	4.107 72	−3.299 69	−39.879 81	221.68240

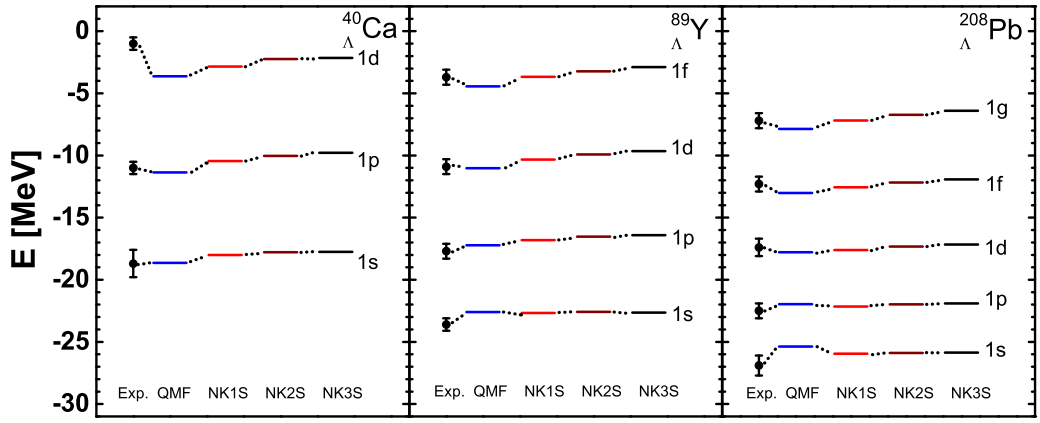

FIG. 2. The results of theoretical calculation for energy levels of Λ hyperon for $^{40}_{\Lambda}$Ca, $^{89}_{\Lambda}$Y, and $^{208}_{\Lambda}$Pb by QMF-NK1S, QMF-NK2S, and QMF-NK3S, compared with the experimental data and the results in the previous QMF model without pion and gluon effects.

as $m_\sigma = 550$ MeV, $m_\omega = 783$ MeV, and $m_\rho = 763$ MeV. g^u_σ, g_ω, g_ρ, g_2, g_3, and c_3 for the normal nuclei have been obtained by fitting the properties of finite nuclei [56].

In the present calculation, we adopt the quark model value of the tensor coupling between ω and hyperons [20,21], $f^H_\omega = -g^H_\omega$, which is important to produce small spin-orbit spitting of hypernuclei. Only the coupling constants between ω and hyperons need to conform. They will be determined via the magnitudes of single hyperon potentials at nuclear saturation density in nuclear matter. The single Λ and Ξ potentials in nuclear matter are fixed as $U_\Lambda = -30$ MeV and $U_\Xi = -12$ MeV at nuclear saturation density respectively, following the existing experimental data about Λ and Ξ hypernuclei. Based on these choices, the single Λ and Ξ potentials in Pb hypernuclei are also calculated to check the validity of g^H_ω. Finally, we obtain three parameter sets about vector coupling constants corresponding to u quark masses $m_u = 250$ MeV, $m_u = 300$ MeV, and $m_u = 350$ MeV, and these parameter sets are listed Table IV. For convenience, we name the first parameter set ($m_u = 250$ MeV) in Table IV as QMF-NK1S, the second one ($m_u = 300$ MeV) as QMF-NK2S, and the third one ($m_u = 350$ MeV) as QMF-NK3S.

The ratios of g^H_ω/g_ω for Λ and Ξ hyperons in QMF-NK1S, QMF-NK2S, and QMF-NK3S do not satisfy the suggestions from simple quark counting rules as 2/3 and 1/3 used in our previous work [40,41]. This is because the cubic term of the σ meson and the biquadratic term of ω term are included in the present work, which generate larger values of g^u_σ and g_ω. The corresponding g^H_ω becomes larger to provide a more repulsive vector potential.

In Fig. 2, the energy levels given by theoretical calculation for the Λ hyperon in three single-Λ hypernuclei, $^{40}_{\Lambda}$Ca, $^{89}_{\Lambda}$Y, and $^{208}_{\Lambda}$Pb, within QMF-NK1S, QMF-NK2S, and QMF-NK3S parameter sets, are compared with the experimental data [62]. Here, we should make a statement that the single-Λ binding energies listed in a recent review article [62] are not the same as the well-known data summarized by Hashimoto and Tamura [63], since they revised these data with the latest experimental information on light hypernuclei from the past few years. The results from our previous QMF calculation without pion and gluon corrections [40] are also given for comparison. We find that the energy levels of the $1d$ state in $^{40}_{\Lambda}$Ca are largely improved in the present model compared with those from the QMF model without pion and gluon corrections. In $^{89}_{\Lambda}$Y and $^{208}_{\Lambda}$Pb, all energy levels are refined in the present calculations to accord better with experimental data. Generally speaking, the Λ energy levels as a whole in QMF-NK3S set are larger than those in QMF-NK1S. This is related to the coupling

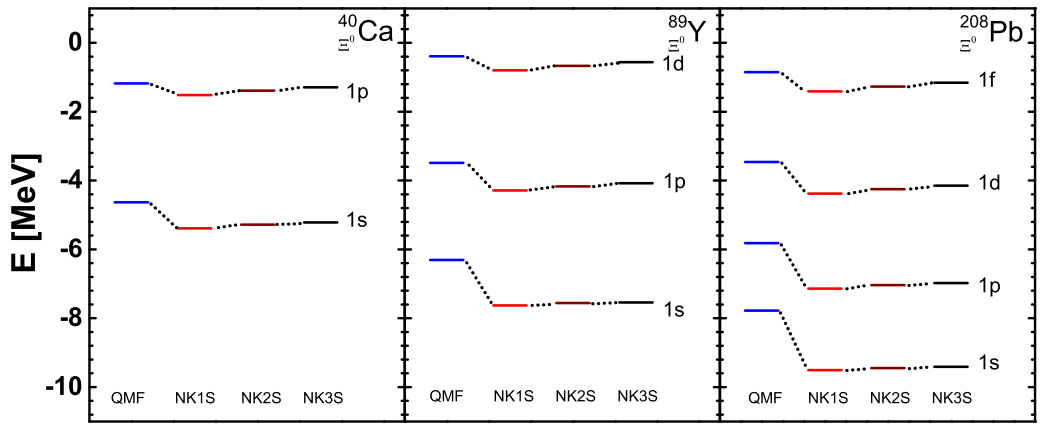

FIG. 3. The results of theoretical calculation for energy levels of Ξ^0 hyperon for $^{40}_{\Xi^0}$Ca, $^{89}_{\Xi^0}$Y, and $^{208}_{\Xi^0}$Pb by QMF-NK1S, QMF-NK2S, and QMF-NK3S, compared with the results in our previous QMF model without pion and gluon corrections.

TABLE V. Energy levels (in MeV) of hyperons for ${}^{40}_{Y}$Ca, ${}^{89}_{Y}$Y, and ${}^{208}_{Y}$Pb by QMF-NK3S in the present model, compared with the experimental data.

	${}^{40}_{\Lambda}$Ca (Expt.)	${}^{40}_{\Lambda}$Ca	${}^{40}_{\Xi}$Ca	${}^{89}_{\Lambda}$Y (Expt.)	${}^{89}_{\Lambda}$Y	${}^{89}_{\Xi}$Y	${}^{208}_{\Lambda}$Pb (Expt.)	${}^{208}_{\Lambda}$Pb	${}^{208}_{\Xi}$Pb
$1s_{1/2}$	-18.7 ± 1.1	-17.76	-5.22	-23.6 ± 0.5	-22.64	-7.54	-26.9 ± 0.8	-25.86	-9.41
$1p_{3/2}$		-9.99	-1.32		-16.53	-4.11		-21.95	-6.99
$1p_{1/2}$	-11.0 ± 0.5	-9.78	-1.29	-17.7 ± 0.6	-16.41	-4.08	-22.5 ± 0.6	-21.90	-6.98
$1d_{5/2}$		-2.42			-9.88	-0.60		-17.27	-4.18
$1d_{3/2}$	-1.0 ± 0.5	-2.15		-10.9 ± 0.6	-9.65	-0.56	-17.4 ± 0.7	-17.16	-4.15
$1f_{7/2}$					-3.19			-12.10	-1.19
$1f_{5/2}$				-3.7 ± 0.6	-2.89		-12.3 ± 0.6	-11.92	-1.16
$1g_{9/2}$								-6.66	
$1g_{7/2}$							-7.2 ± 0.6	-6.40	

constants without strangeness degree of freedom. For example, the binding energy of ^{208}Pb from QMF-NK3 is smaller than that from QMF-NK1, as shown in Ref. [56].

Encouraged by the good agreements of Λ hypernuclei data in our present model, we start to calculate the energy levels of Ξ^0 hypernuclei in the same framework, to serve as a reference for future experiments. The single-particle energy levels of Ξ^0 for ${}^{40}_{\Xi^0}$Ca, ${}^{89}_{\Xi^0}$Y,and ${}^{208}_{\Xi^0}$Pb are collected in Fig. 3. We can find that the results obtained from present model are deeper than that from the QMF model without pion and gluon corrections.

Single-Λ and single-Ξ^0 energies of these hypernuclei within the QMF-NK3S set and the corresponding experimental data are listed in detail in Table V. The differences of single-Λ binding energies in theory and experiment are less than 5% of the experimental values. The spin-orbit splittings of these single-Λ hypernuclei are usually less than 0.3 MeV, since the tensor couplings between vector meson and hyperons are included in this work. The small spin-orbit splittings are in accord with the available experiment data. For single-Ξ^0 hypernuclei, the high angular momentum states do not exist, compared with the corresponding single-Λ hypernuclei, due to small value of the single-Ξ potential at nuclear saturation density. In this case, the deepest bound state of Ξ^0 exists in ${}^{208}_{\Xi^0}$Pb, at about -9.5 MeV.

In Fig. 4, we plot the scalar potential U_S^Λ and vector potential U_V^Λ for the $1s_{1/2}$ Λ state in ${}^{40}_{\Lambda}$Ca, ${}^{89}_{\Lambda}$Y, and ${}^{208}_{\Lambda}$Pb. We find that the scalar potential from the σ meson almost has the same magnitude as the repulsive vector potential from the ω meson. They will cancel with each other and finally generate a total attractive force, whose center part is around 23–30 MeV in ${}^{40}_{\Lambda}$Ca, ${}^{89}_{\Lambda}$Y, and ${}^{208}_{\Lambda}$Pb. The larger u quark mass will provide more attractive scalar and repulsive vector potentials, which is related to the smaller effective Λ mass and larger vector coupling constant in the QMF-NK3S parameter set.

Similarly, the scalar and vector potentials of the single-Ξ^0 hypernuclei $1s_{1/2}$ Ξ^0 state are given in Fig. 5. They are just about 50% in Λ hypernuclei. The scalar and vector potentials finally produce attractive potentials at the center part of Ξ^0 hypernuclei, whose values are about 7–12 MeV in ${}^{40}_{\Xi^0}$Ca, ${}^{89}_{\Xi^0}$Y, and ${}^{208}_{\Xi^0}$Pb.

In Fig. 6, the binding energies of single-Λ hypernuclei are systematically calculated from ${}^{16}_{\Lambda}$O to ${}^{208}_{\Lambda}$Pb within the QMF-NK3S parameter set at different spin-orbit states and are compared with the experimental data [62]. It can be found that the experiment observables are reproduced very well in the QMF model, including pion and gluon corrections. If pion and gluon corrections are not included [40], the Λ binding energies at s and p spin-orbit states are in accord with experimental data; however, there were few-MeV differences of Λ binding energies between theoretical results and experimental values above d spin-orbit states. It is conclusive

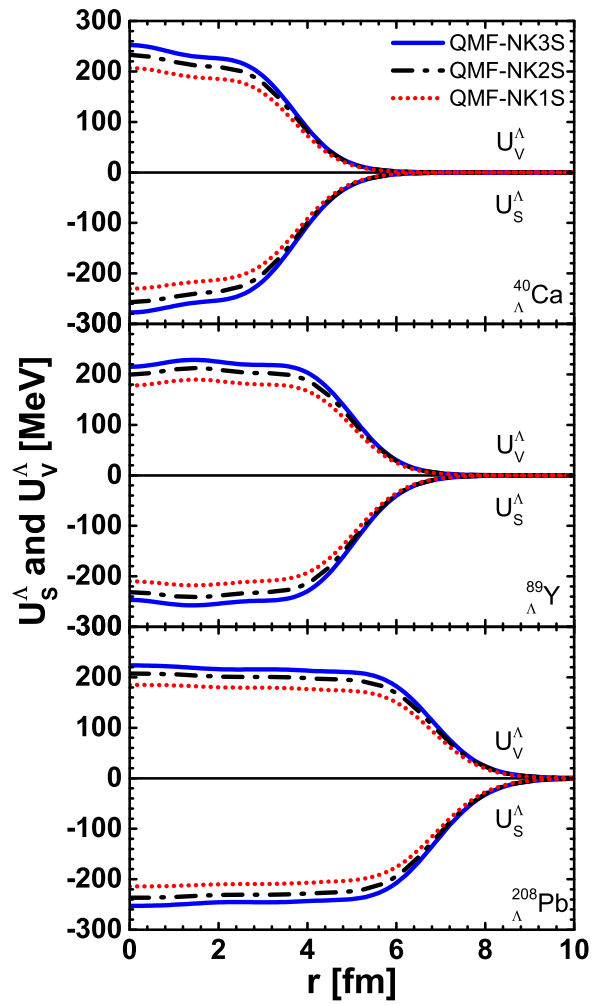

FIG. 4. The scalar and vector potentials, U_S^Λ and U_V^Λ, for the $1s_{1/2}$ Λ state in ${}^{40}_{\Lambda}$Ca, ${}^{89}_{\Lambda}$Y, and ${}^{208}_{\Lambda}$Pb by QMF-NK1S, QMF-NK2S, and QMF-NK3S.

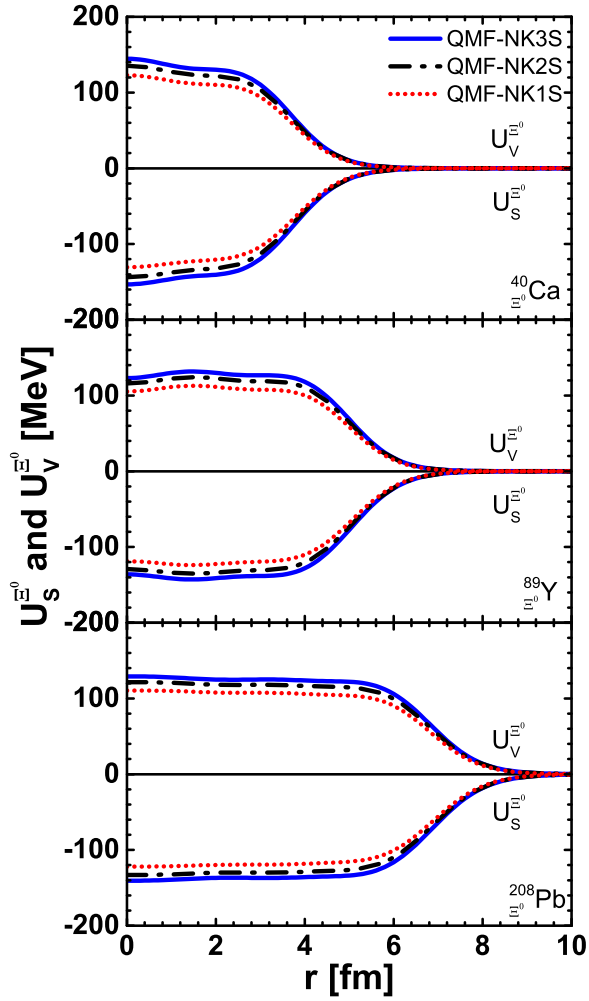

FIG. 5. The scalar and vector potentials, $U_S^{\Xi^0}$ and $U_V^{\Xi^0}$, for the $1s_{1/2}$ Ξ^0 state in $^{40}_{\Xi^0}$Ca, $^{89}_{\Xi^0}$Y, and $^{208}_{\Xi^0}$Pb by QMF-NK1S, QMF-NK2S, and QMF-NK3S.

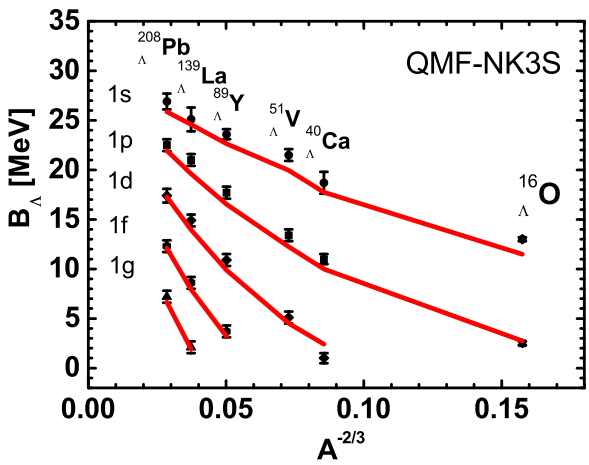

FIG. 6. Systematic calculations of the binding energies of Λ hypernuclei with the QMF-NK3S parameter set compared with the experimental data.

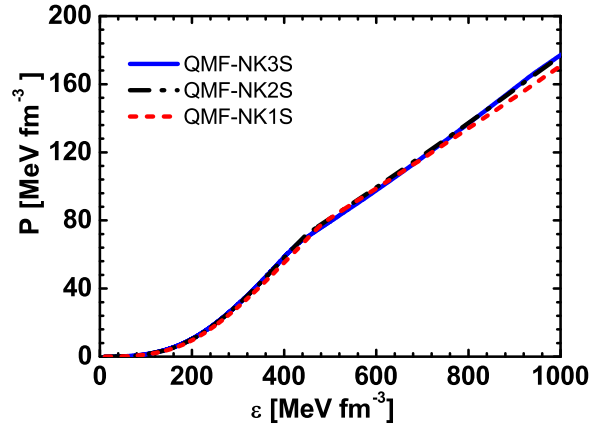

FIG. 7. Pressures of β equilibrated matter as functions of the energy density, for QMF-NK1S, QMF-NK2S, and QMF-NK3S parameter sets.

that the QMF model including the pion and gluon corrections can improve the description of Λ hypernuclei from the quark level.

C. Properties of neutron stars

Once the properties of single Λ and Ξ^0 hypernuclei are determined by the QMF model with pion and gluon corrections, strange nuclear matter and neutron stars can be studied in the present framework. For neutron star matter, all baryons and leptons stay in a charge neutrality and β equilibrium environment. Furthermore, Σ hyperons also have the probability to appear in neutron star matter, although there is no evidence of existing of single-Σ hypernuclei from experiments to date. To make the present discussion simpler, the coupling constant between the ω meson and Σ hyperon is taken to be same value as g_ω^Λ. Furthermore, the ρ meson may play an important role in neutron star matter, whose coupling constants related to hyperons are chosen as $g_\rho^H = g_\rho$. After solving the corresponding equations, the energy density and pressure of neutron star matter can be obtained as shown in Fig. 7 within QMF-NK1S, QMF-NK2S, and QMF-NK3S sets. At low energy density, the pressures of three parameter sets are almost identical, since the behaviors of neutron star matter at low density are decided by the properties of finite nuclei; meanwhile, the hyperons do not appear due to their larger chemical potentials. With energy density increasing, the pressure of QMF-NK1S becomes a little bit different from those of QMF-NK2S and QMF-NK3S for hyperon appearance.

Besides the relation between energy density and pressure, the fractions of leptons and baryons in neutron star matter as functions of total baryon density are also given in Fig. 8 with different parameter sets. The direct Urca processes will happen above the densities $\rho_B = 0.287, 0.244$, and 0.229 fm^{-3} in QMF-NK1S, QMF-NK2S, and QMF-NK3S, respectively, which are higher than the case without pion and gluon corrections, $\rho_B = 0.21$ fm^{-3}. This satisfies the constraint of astrophysical observations, where the cooling process does not occur at too low proton density. Furthermore, both Λ

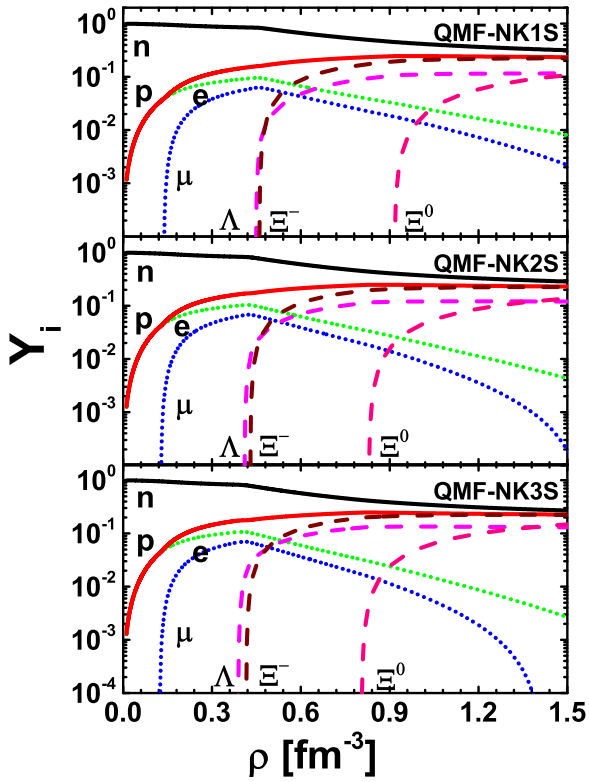

FIG. 8. Fractions of leptons and baryons in neutron star matter as functions of total baryon density, for QMF-NK1S, QMF-NK2S, and QMF-NK3S parameter sets.

and Ξ^- hyperons appear around two times saturation density. Ξ^0 hyperons exist above $\rho_B = 0.9$ fm^{-3}. At high density, the fraction of Ξ^- hyperons approaches that of protons. Meanwhile, the fraction of Λ hyperons is suppressed by Ξ^- hyperons. In total, the appearance of hyperons occurs earlier at larger u quark mass.

By using the EOS of neutron star matter to solve the TOV equation, the properties of neutron stars, such as the masses as functions of central density and radius, are obtained in Fig. 9. The maximum masses are $2.09M_\odot$ to $2.14M_\odot$ generated by

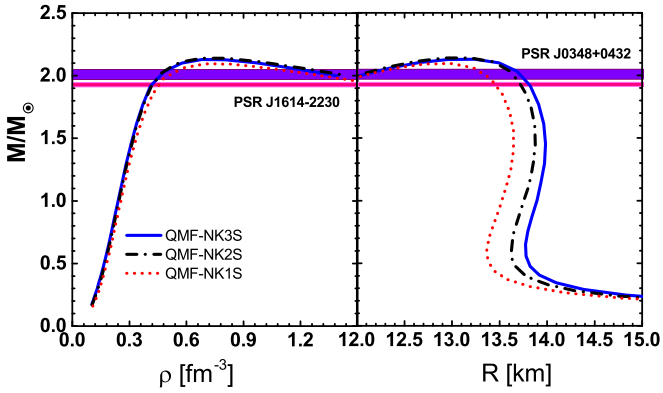

FIG. 9. The masses of neutron stars as functions of density and radius, for QMF-NK1S, QMF-NK2S, and QMF-NK3S parameter sets.

QMF-NK1S to QMF-NK3S, respectively. These results are in accord with recent astronomical observations of two massive neutron stars, PSR J1614-2230 ($1.928 \pm 0.017\,M_\odot$) [25,26] and PSR J0348+0432 ($2.01 \pm 0.04\,M_\odot$) [27]. Moreover, the hyperons Λ and Ξ can exist in the core region of a neutron star. The densities corresponding to maximum masses are around $\rho_B = 0.7$ fm^{-3}. The radii of these neutron stars are distributed from 13.0 to 13.2 km. They are larger than the constraint region determined by Hebeler *et al.* [64,65] around 11 km, but smaller than values from the MQMC framework. Actually, the radius of a neutron star still has not been measured directly. Comparing our previous work with a QMF model without pion and gluon corrections [41], the description of properties of neutron stars is largely improved to satisfy the constraint of observations in the present QMF parameter sets.

IV. CONCLUSION

We have studied the properties of single Λ and Ξ^0 hypernuclei and neutron stars with hyperons in terms of a quark mean field (QMF) model including pion and gluon corrections, where the baryons are composed of three independent relativistic quarks confined by a harmonic oscillator potential mixing with scalar and vector components. Corrections due to the center-of-mass motion and pionic and gluonic exchanges were considered in calculating properties of baryons perturbatively. The baryon-baryon interactions were generated by exchanging σ, ω, and ρ mesons between quarks of different baryons in a mean field approximation.

The strengths of s quark confinement potentials and constituent quark mass were determined by fitting free baryon masses of Λ, Σ^0, and Ξ^0 hyperons with a least-squares fitting method as a whole. The coupling constants between u,d quarks and mesons were already obtained in our previous work about normal nuclei. Those between s quarks and mesons were determined through the potentials of ΛN and ΞN at nuclear saturation density, as $U_\Lambda = -30$ MeV and $U_\Xi = -12$ MeV, respectively. Finally, we obtained three parameter sets corresponding to u quark mass: $m_u = 250$ MeV, $m_u = 300$ MeV, and $m_u = 350$ MeV, named QMF-NK1S, QMF-NK2S, and QMF-NK3S.

Energy levels of a single Λ hyperon for three hypernuclei, ${}^{40}_{\Lambda}$Ca, ${}^{89}_{\Lambda}$Y, and ${}^{208}_{\Lambda}$Pb, were calculated. The results were very consistent with the experiment observations and were largely improved comparing to those from the previous QMF model without pion and gluon corrections, especially for high angular momentum states. Meanwhile, energy levels of a single Ξ^0 hyperon in ${}^{40}_{\Xi^0}$Ca, ${}^{89}_{\Xi^0}$Y, and ${}^{208}_{\Xi^0}$Pb were also obtained. The results for Ξ^0 hypernuclei could serve as a reference for future experiments. The Λ binding energies from ${}^{16}_{\Lambda}$O to ${}^{208}_{\Lambda}$Pb were also compared systematically to the experimental data, and agree with them very well.

Finally, properties of neutron stars were studied in the present framework. The coupling constants of Λ and Ξ hyperons were kept at the same values used in hypernuclei. The coupling constant between the ω meson and Σ hyperon was chosen to be the same value as for the Λ hyperon. It was found that the Λ and Ξ^- hyperons started to appear in neutron stars at two times nuclear saturation density and

Ξ^0 hyperons at five times nuclear saturation density. The Σ hyperons did not exist in the cores of neutron stars in this work. The maximum masses of neutron stars were around $2.09M_\odot$ to $2.14M_\odot$ within the QMF-NK1S, QMF-NK2S, and QMF-NK3S sets, which satisfied the requirement of recent astronomical observations about massive neutron stars. The corresponding radii of neutron stars were about 13 km.

The present QMF model including the pion and gluon corrections could describe properties of both hypernuclei and neutron stars, and satisfy the constraints of experimental data. In this work, to simplify our study, the charged Ξ^- and double Λ hypernuclei were not discussed; however, many experiments have been proposed to study their properties in large facilities. The related work is in progress.

ACKNOWLEDGMENTS

This work was supported in part by the National Natural Science Foundation of China (Grants No. 11375089 and No. 11405090) and the Fundamental Research Funds for the Central Universities.

[1] A. Feliciello and T. Nagae, Rep. Prog. Phys. **78**, 096301 (2015).
[2] S. Aoki *et al.*, Prog. Theor. Phys. **89**, 493 (1993)
[3] M. Yamaguchi, K. Tominaga, Y. Yamamoto, and T. Ueda, Prog. Theor. Phys. **105**, 627 (2001).
[4] K. Nakazawa *et al.*, Prog. Theor. Exp. Phys. **2015**, 033D02 (2015).
[5] T. Gogami *et al.*, Phys. Rev. C **93**, 034314 (2016).
[6] M. Danysz *et al.*, Nucl. Phys. **49**, 121 (1963).
[7] D. J. Prowse *et al.*, Phys. Rev. Lett. **17**, 782 (1966).
[8] S. Aoki *et al.*, Prog. Theor. Phys. **85**, 1287 (1991).
[9] G. B. Franklin, Nucl. Phys. A **585**, 83 (1995).
[10] H. Takahashi *et al.*, Phys. Rev. Lett. **87**, 212502 (2001).
[11] A. Gal, Int. J. Mod. Phys. E **19**, 2301 (2010).
[12] E. Botta, T. Bressani, and G. Garbarino, Eur. Phys. J. A **48**, 41 (2012).
[13] H. Tamura, Prog. Theor. Exp. Phys. **2012**, 02B012 (2012).
[14] E. Hiyama and T. Yamada, Prog. Part. Nucl. Phys. **63**, 339 (2009).
[15] N. Guleria, S. K. Dhiman, and R. Shyam, Nucl. Phys. A **886**, 71 (2012).
[16] A. Li, E. Hiyama, X.-R. Zhou, and H. Sagawa, Phys. Rev. C **87**, 014333 (2013).
[17] H.-J. Schulze and T. Rijken, Phys. Rev. C **88**, 024322 (2013), and references therein.
[18] J. W. Cui, X. R. Zhou, and H.-J. Schulze, Phys. Rev. C **91**, 054306 (2015).
[19] X. R. Zhou, E. Hiyama, and H. Sagawa, Phys. Rev. C **94**, 024331 (2016).
[20] Y. Sugahara and H. Toki, Prog. Theor. Phys. **92**, 803 (1994).
[21] H. Shen, F. Yang, and H. Toki, Prog. Theor. Phys. **115**, 325 (2006).
[22] R. L. Xu, C. Wu, and Z. Z. Ren, J. Phys. G: Nucl. Part. Phys. **39**, 085107 (2012).
[23] T. T. Sun, E. Hiyama, H. Sagawa, H.-J. Schulze, and J. Meng, Phys. Rev. C **94**, 064319 (2016).
[24] Y. Tanimura and K. Hagino, Phys. Rev. C **85**, 014306 (2012).
[25] P. B. Demorest, T. Pennucci, S. M. Ransom, M. S. E. Roberts, and J. W. T. Hessels, Nature (London) **467**, 1081 (2010).
[26] E. Fonseca *et al.*, Astrophys. J. **832**, 167 (2016).
[27] J. Antoniadis, P. C. C. Freire, N. Wex, T. M. Tauris, R. S. Lynch *et al.*, Science **340**, 1233232 (2013).
[28] S. Weissenborn, D. Chatterjee, and J. Schaffner-Bielich, Phys. Rev. C **85**, 065802 (2012).
[29] M. Oertel, C. Providência, F. Gulminelli, and Ad. R. Raduta, J. Phys. G: Nucl. Part. Phys. **42**, 075202 (2015).
[30] Y. Yamamoto, T. Furumoto, N. Yasutake, and T. A. Rijken, Phys. Rev. C **88**, 022801 (2013); **90**, 045805 (2014).
[31] P. K. Panda, A. Mishra, J. M. Eisenberg, and W. Greiner, Phys. Rev. C **56**, 3134 (1997).
[32] P. K. Panda, R. Sahu, and C. Das, Phys. Rev. C **60**, 038801 (1999).
[33] P. K. Panda, G. Krein, D. P. Menezes, and C. Providencia, Phys. Rev. C **68**, 015201 (2003).
[34] P. K. Panda, D. P. Menezes, and C. Providencia, Phys. Rev. C **69**, 025207 (2004).
[35] P. K. Panda, A. M. S. Santos, D. P. Menezes, and C. Providencia, Phys. Rev. C **85**, 055802 (2012).
[36] K. Saito, K. Tsushima, and A. W. Thomas, Prog. Part. Nucl. Phys. **58**, 1 (2007).
[37] H. Toki, U. Meyer, A. Faessler, and R. Brockmann, Phys. Rev. C **58**, 3749 (1998).
[38] H. Shen and H. Toki, Phys. Rev. C **61**, 045205 (2000).
[39] H. Shen and H. Toki, Nucl. Phys. A **707**, 469 (2002).
[40] J. N. Hu, A. Li, H. Shen, and H. Toki, Prog. Theor. Exp. Phys. **2014**, 013D02 (2014).
[41] J. N. Hu, A. Li, H. Toki, and W. Zuo, Phys. Rev. C **89**, 025802 (2014).
[42] P. Wang, Z. Y. Zhang, Y. W. Yu, R. K. Su, and H. Q. Song, Nucl. Phys. A **688**, 791 (2001).
[43] P. Wang, H. Guo, Z. Y. Zhang, Y. W. Yu, R. K. Su, and H. Q. Song, Nucl. Phys. A **705**, 455 (2002).
[44] P. Wang, V. E. Lyubovitskij, T. Gutsche, and A. Faessler, Phys. Rev. C **67**, 015210 (2003).
[45] P. Wang, D. B. Leinweber, A. W. Thomas, and A. G. Williams, Nucl. Phys. A **744**, 273 (2004).
[46] P. Wang, D. B. Leinweber, A. W. Thomas, and A. G. Williams, Phys. Rev. C **70**, 055204 (2004).
[47] P. Wang, D. B. Leinweber, A. W. Thomas, and A. G. Williams, Nucl. Phys. A **748**, 226 (2005).
[48] J. J. Aubert *et al.* (EMC Collaboration), Phys. Lett. B **123**, 275 (1983).
[49] G. Krein, A. W. Thomas, and K. Tsushima, Nucl. Phys. A **650**, 313 (1999).
[50] J. R. Stone, P. A. M. Guichon, H. H. Matevosyan, and A. W. Thomas, Nucl. Phys. A **792**, 341 (2007).
[51] D. L. Whittenbury, J. D. Carroll, A. W. Thomas, K. Tsushima, and J. R. Stone, Phys. Rev. C **89**, 065801 (2014).
[52] S. Nagai, T. Miyatsu, K. Saito, and K. Tsushima, Phys. Lett. B **666**, 239 (2008).

[53] N. Barik, R. N. Mishra, D. K. Mohanty, P. K. Panda, and T. Frederico, Phys. Rev. C **88**, 015206 (2013).
[54] R. N. Mishra, H. S. Sahoo, P. K. Panda, N. Barik, and T. Frederico, Phys. Rev. C **92**, 045203 (2015).
[55] R. N. Mishra, H. S. Sahoo, P. K. Panda, N. Barik, and T. Frederico, Phys. Rev. C **94**, 035805 (2016).
[56] X. Y. Xing, J. N. Hu, and H. Shen, Phys. Rev. C **94**, 044308 (2016), and references therein.
[57] J. R. Oppenheimer and G. M. Volkoff, Phys. Rev. **55**, 374 (1939).
[58] R. C. Tolman, Phys. Rev. **55**, 364 (1939).
[59] M. B. Parappilly, P. O. Bowman, U. M. Heller, D. B. Leinweber, A. G. Williams, and J. B. Zhang, Phys. Rev. D **73**, 054504 (2006).
[60] G. Burgio, M. Schröck, H. Reinhardt, and M. Quandt, Phys. Rev. D **86**, 014506 (2012).
[61] C. Patrignani *et al.* (Particle Data Group), Chin. Phys. C **40**, 100001 (2016).
[62] A. Gal, E. V. Hungerford, and D. J. Millener, Rev. Mod. Phys. **88**, 035004 (2016).
[63] O. Hashimoto and H. Tamura, Prog. Part. Nucl. Phys. **57**, 564 (2006).
[64] K. Hebeler, J. M. Lattimer, C. J. Pethick, and A. Schwenk, Phys. Rev. Lett. **105**, 161102 (2010).
[65] K. Hebeler, J. M. Lattimer, C. J. Pethick, and A. Schwenk, Astrophys. J. **773**, 11 (2013).